ACS OMEGA

http://pubs.acs.org/journal/acsodf

Article

Electronic and Magnetic Properties of the Graphene/Y/Co(0001) Interfaces: Insights from the Density Functional Theory Analysis

Wenxuan Yue, Qilin Guo, Yuriy Dedkov,* and Elena Voloshina*

Cite This: *ACS Omega* 2022, 7, 7304−7310

Read Online

ACCESS | Metrics & More | Article Recommendations | Supporting Information

ABSTRACT: The effect of Y intercalation on the atomic, electronic, and magnetic properties of the graphene/Co(0001) interface is studied using state-of-the-art density functional theory calculations. Different structural models of the graphene/Y/Co(0001) interface are considered: (i) graphene/Y/Co(0001), (ii) graphene/1ML-YCo_2/Co(0001), and (iii) graphene/bulk-like-YCo_2(111). It is found that the interaction strength between graphene and the substrate is strongly affected by the presence of Y at the interface and the electronic structure of graphene (doping and the appearance of the energy gap) is defined by the Y concentration. For the Co-terminated interfaces between graphene and the metallic support in the considered systems, the electronic structure of graphene is strongly disturbed, leading to the absence of the linear dispersion for the graphene π band; in the case of the Y-terminated interfaces, a graphene layer is strongly *n*-doped, but the linear dispersion for this band is preserved. Our calculations show that the magnetic anisotropy for the magnetic atoms at the graphene/metal interface is strongly affected by the adsorption of a graphene layer, giving a possibility for one to engineer the magnetic properties of the graphene/ferromagnet systems.

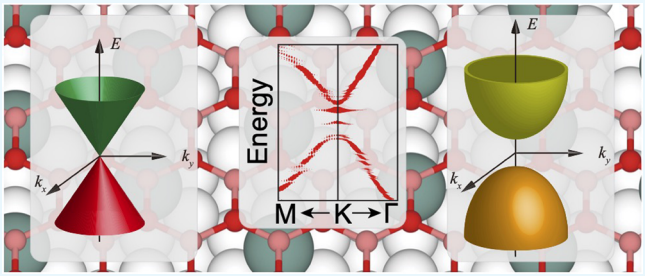

INTRODUCTION

Graphene (gr), a single atomic layer of graphite, has been in the focus of a large number of experimental and theoretical studies due to its unique physical properties.[1−4] Many of these properties are defined by the behavior of the graphene-derived π states in the vicinity of the Fermi level (E_F), which have a linear dispersion around the *K* points of the graphene Brillouin zone. This also leads to the zero-level density of states (DOS) at E_F attributing graphene to a class of solids called semimetals. Such properties make graphene an ideal material for the fabrication of different low-dimensional devices, which were already made or proposed.[5,6] Any application of graphene in the real electron- or spin-transport devices requires that at some point a graphene layer is contacted by a metallic or semiconducting channel. When graphene is considered on an arbitrary support, one can expect, in the general case, a strong modification of its valence band electronic structure. Here, several factors have to be taken into account: charge transfer from/onto graphene-derived π states, hybridization of the electronic valence band states of graphene and the support, and the lattice match between the graphene and metallic or semiconducting surface.[7−11] These factors determine the behavior of the π states in the vicinity of E_F as well as the appearance of an energy gap in the spectrum of the graphene-derived electronic states at the so-called Dirac point, E_D.[12−16]

When graphene is brought in contact with a ferromagnetic (FM) material (as in the particular case of a graphene/metal interface), a magnetic moment can be raised in carbon atoms[16−19] together with the appearance of a spin polarized state at the Fermi level.[20,21] On the other hand, the ferromagnet experiences a huge interfacial magnetic anisotropy[22,23] and its magnetic configuration changes dramatically.[24] The electronic structure of the gr/FM interface can be further modified via intercalation of different species with the aim to prepare different graphene-based heterostructures. Here, e.g., the intercalation of Fe leads to an increase of the induced magnetic moment in graphene;[18,25] the intercalation of noble metals and halogens decouples graphene from the FM material with a controllable modification of the graphene band structure around the Dirac point.[26−28] The intercalation of oxygen in gr/Ni and gr/Co interfaces leads to the formation of thin layers of antiferromagnetic (AFM) metal oxides and the resulting epitaxial graphene-protected AFM/FM systems, which can be used in future spintronics applications.[29−31] Moreover, the insertion of other magnetic atoms with open d-shells into the gr/metal interface might lead to the formation of ordered gr/FM-alloy systems with interesting properties.[32−35] Therefore, the studies of such gr/FM hybrid systems have a huge implications from both the basic scientific and technological standpoints.

Received: December 17, 2021
Accepted: February 11, 2022
Published: February 17, 2022

https://doi.org/10.1021/acsomega.1c07136
ACS Omega 2022, 7, 7304−7310

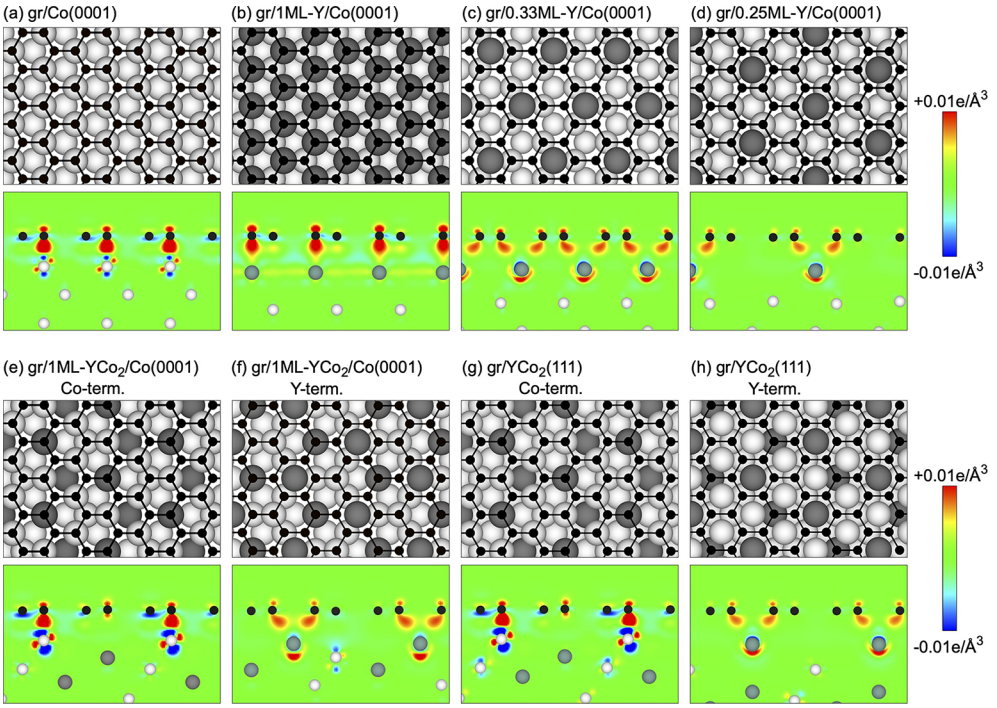

Figure 1. Top and side views of different Y-based intercalation structures: (a) parent gr/Co(0001), (b) gr/1ML-Y/Co(0001), (c) gr/0.33ML-Y/Co(0001), (d) gr/0.25ML-Y/Co(0001), (e) gr/1ML-YCo_2/Co(0001) with Co-terminated YCo_2(111), (f) gr/1ML-YCo_2/Co(0001) with Y-terminated YCo_2(111), (g) gr/bulk-like-YCo_2(111) with Co-terminated YCo_2(111), and (h) gr/bulk-like-YCo_2(111) with Y-terminated YCo_2(111). Spheres of different sizes and colors represent atoms of different types (C: black; Co: gray; Y: dark gray). Side views for all structures are taken along the graphene arm-chair edge, and they are overlaid with electron charge difference maps $\Delta\rho(\mathbf{r}) = \rho_{gr/s}(\mathbf{r}) - (\rho_{gr}(\mathbf{r}) + \rho_s(\mathbf{r}))$ with gr: graphene; s: substrate. $\Delta\rho$ is color coded as blue (−0.01 e/Å^3), green (0), and red (+0.01 e/Å^3).

Table 1. Results for the Atomic Structure of the Graphene/Substrate Interface Models and for the Clean Metal Surfaces[a]

system	E_{int}	d_0	d_1	d_2	m_C	m_{Co}	m_Y	MAE
gr/Co(0001)	−214	2.09	1.92	1.93	−0.043/0.038	1.51/1.63		0.34
gr/1ML-Y/Co(0001)	−322	2.55	2.61	1.93	−0.02/0.01	1.54/1.64	−0.10	1.35
gr/0.33ML-Y/Co(0001)	−242	2.28	2.31	1.95	0.01/0.01	1.50/1.64	−0.11	1.11
gr/0.25ML-Y/Co(0001)	−178	2.32	2.19	1.95	−0.00/0.00	1.44/1.63	−0.18	−1.10
gr/1ML-YCo_2/Co(0001)[b]	−195	2.01	1.16	0.77	−0.03/0.02/−0.02	1.27/1.53	−0.28	−1.38
gr/1ML-YCo_2/Co(0001)[c]	−209	2.27	0.93	0.85	−0.01/0.01/0.01	1.28/1.53	−0.25	−1.25
gr/YCo_2(111)[b]	−210	2.03	1.19	0.77	−0.02/0.01/−0.03	1.27/0.02	−0.15	−0.58
gr/YCo_2(111)[c]	−147	2.34	1.73	1.53	−0.00/0.00/−0.01	1.11/0.01	−0.26	0.33

[a] E_{int} (meV/C atom) is the interaction energy, defined as $E_{int} = E_{gr/s} - (E_{gr} + E_s)$, where $E_{gr/s}$ is the total energy of the graphene/substrate system and E_{gr} and E_s are the energies of the fragments at the same coordinates as in the graphene/substrate system; d_0 (in Å) is the mean distance between the graphene overlayer and the interface substrate layer; d_1 (in Å) is the mean distance between the interface substrate layer and the second substrate layer; d_2 (in Å) is the mean distance between the second and third substrate layers; m_C (μ_B) is the interface C spin magnetic moment (several values for the nonequivalent carbon atoms are indicated); m_{Co} (μ_B) is the Co spin magnetic moment (two values are given for the interface/bulk atoms); m_Y (μ_B) is the interface Y spin magnetic moment; MAE (meV/u.c.) is the out-of-plane magnetic anisotropy energy. [b] Co termination of YCo_2(111). [c] Y termination of YCo_2(111).

Here, we present the systematic density functional theory (DFT) studies of the electronic and magnetic properties of the systems obtained upon intercalation of yttrium (Y, atomic electronic configuration [Kr] $5s^2$ $4d^1$) in gr/Co(0001). Our study is motivated by the possibility to intercalate Y in gr/Co(0001) and to form a graphene-protected FM-YCo_2 layer on top of the paramagnetic (PM) bulk. The existence of the 1ML-FM-YCo_2/PM-YCo_2, where unwanted electron scattering can be avoided, is confirmed by the previous works.[36,37] Different structural models of the gr/Y/Co(0001) interface that can be formed after Y-intercalation are considered, which include several concentrations of Y-intercalant and the possible formation of an YCo_2 alloy at the gr/metal interface. We found that in the case of the sharp gr/Y/Co(0001) interface the presence of the realistic amount of Y preserves the linear dispersion for the strongly *n*-doped graphene-derived π-bands. In the case of the YCo_2 alloy formation at the interface, the adsorption of graphene on the Co-terminated alloy leads to the strong hybridization of the graphene π and Co 3d states, similar to the adsorption of graphene on Co(0001). For the Y-terminated gr/YCo_2 interface, the linear dispersion is preserved, leading to the formation of a strongly *n*-doped graphene. Our theoretical findings can be of interest for the future spectroscopic experiments of the discussed systems and also in the studies of the spin-related phenomena in the gr/FM

https://doi.org/10.1021/acsomega.1c07136
ACS Omega 2022, 7, 7304−7310

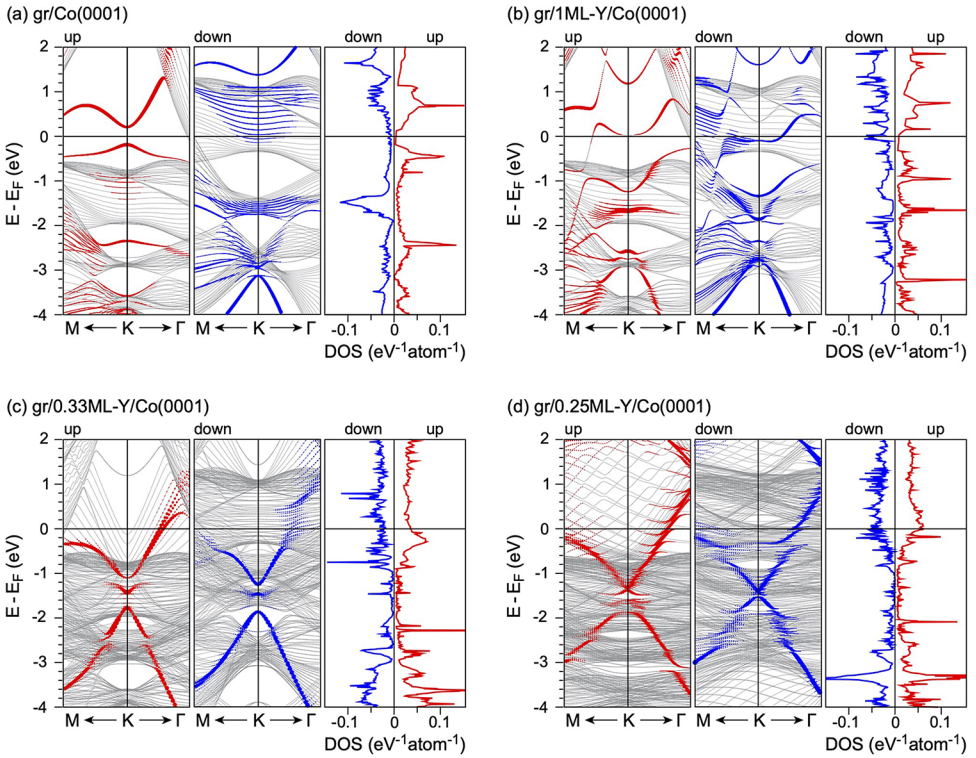

Figure 2. Spin-resolved band structures and C-p_z-projected density of states for (a) parent gr/Co(0001), (b) gr/1ML-Y/Co(0001), (c) gr/0.33ML-Y/Co(0001), and (d) gr/0.25ML-Y/Co(0001). Band structures are presented around the *K* point for the graphene-derived (1 × 1) Brillouin zone. The weight of the graphene-derived p_z character is highlighted by the size of filled circles superimposed with the plot of the band structure.

systems and for the discussion of the possible realization of different spintronics devices.

RESULTS AND DISCUSSION

As was shown in the previous experimental and theoretical works[21,38−40] and also confirmed by the present results (see Table S1 and Figure S1), a single graphene layer is adsorbed on Co(0001) in the so-called *top*−*fcc* configuration, where one carbon atom of the graphene unit cell is adsorbed above the Co interface atom and second carbon atom is located at the *fcc* hollow site of the Co(0001) surface (Figure 1a). Such adsorption geometry leads to a small distance of 2.09 Å between graphene and the topmost metal layer (denoted as M(S) further in the text), and the adsorption energy for graphene on Co(0001) is equal to −214 meV/C atom (see Table 1).

The adsorption of graphene on Co(0001) leads to the *n*-doping of graphene due to the charge transfer from Co to graphene (see Figure 1a) with a downward shift of the graphene-derived π states, followed by the strong hybridization of the graphene-π and Co 3d valence band states (Figures 2a and S2). As a result, several hybrid states are formed in the vicinity of E_F with the predominant Co 3d character (Figure S3). As a further consequence of the interaction between graphene and Co valence band states, the magnetic moment on carbon atoms appears as $m(C^{top}) = -0.042\ \mu_B$ and $m(C^{fcc}) = 0.039\ \mu_B$, respectively, indicating a small net magnetic moment in graphene. Simultaneously, the magnetic moment of the interface Co atoms is reduced to 1.51 μ_B (Table 1) compared to the values of 1.73 μ_B and 1.63 μ_B for the clean Co(0001) surface and Co bulk, respectively (also see Figure S4 for the distribution of magnetic moments in all considered systems). This can be assigned to the strong overlap of the electronic states of graphene and Co interface atoms leading to the redistribution of magnetic moments of cobalt interface atoms, as was also previously observed for the gr/Ni(111) system.[17,18,40] Furthermore, the out-of-plane magnetic anisotropy energy (MAE) is increased from 0.15 meV/u.c. for a clean Co(0001) surface to 0.34 meV/u.c. for gr/Co(0001) due to the graphene adsorption and the effect of hybridization between graphene-π and Co 3d orbitals with a predominant *z*-orientation.[40,41]

When considering the intercalation of Y under graphene on Co(0001), several scenarios are possible. Let us start with an assumption that Y atoms form a 2D hexagonal layer commensurate with the (1 × 1)-Co(0001) substrate (Figure S5a−c, Tables S2 and S3). Here, for the gr/1ML-Y/Co(0001) system, in the case of the most energetically favorable configuration, the Y intercalant occupies the *fcc* hollow sites above Co(0001) (Figure 1b). In such a structure, the lateral Y−Y distance is 2.49 Å, which is too short as compared to the respective distance in the bulk Y (3.65 Å) and will be considered only for comparison reasons. In addition, we took into account more realistic concentrations of Y atoms equal to 0.33- and 0.25ML, which correspond to d_{Y-Y} = 4.32 and 4.98 Å, respectively (Figure S5d−f,g−i). In these two cases, Y atoms prefer to occupy the *hcp* hollow sites of the Co(0001) slab so that each Y atom is surrounded by a carbon ring (Figure 1c,d, Tables S2 and S3).

In the case of gr/1ML-Y/Co(0001), graphene is *n*-doped and the formation of the [C^{top}-p_z + M(S)-d_{z^2}] and [C^{fcc}-p_z + M(S)-d_{xz}, -d_{yz}] hybrid states leads to a massive rearrangement of bands (Figures 2b and S6). As a consequence in the

https://doi.org/10.1021/acsomega.1c07136
ACS Omega 2022, 7, 7304−7310

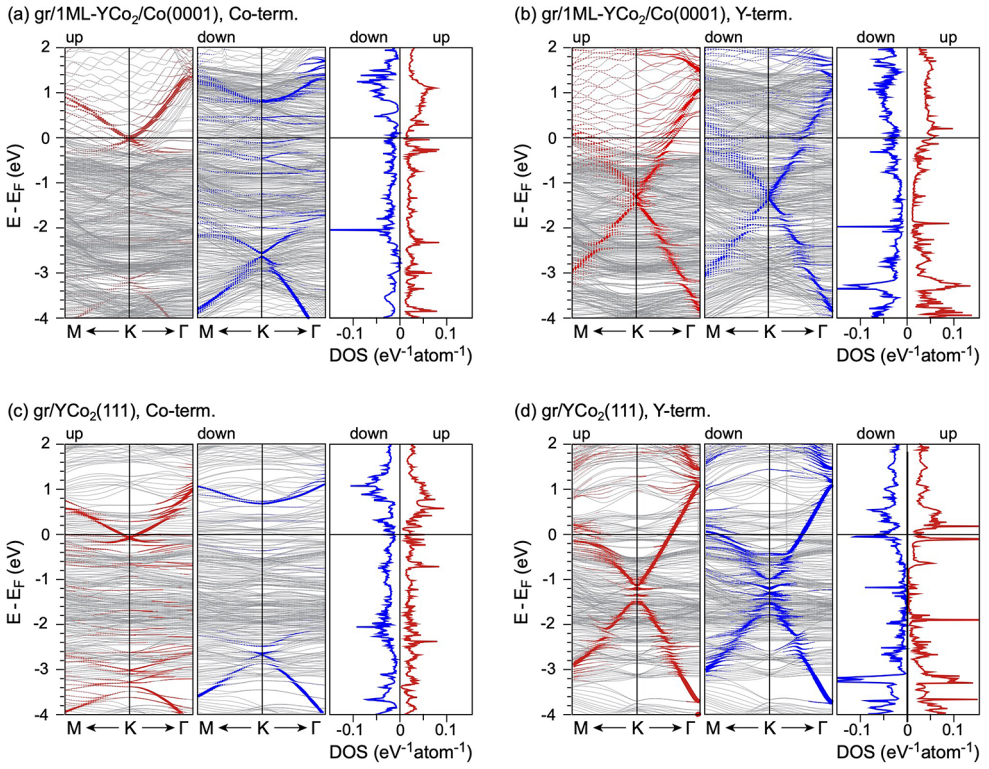

Figure 3. Spin-resolved band structures and C-p_z-projected density of states for (a) gr/1ML-YCo_2/Co(0001) with Co-terminated YCo_2(111), (b) gr/1ML-YCo_2/Co(0001) with Y-terminated YCo_2(111), (c) gr/bulk-like-YCo_2(111) with Co-terminated YCo_2(111), and (d) gr/bulk-like-YCo_2(111) with Y-terminated YCo_2(111). Band structures are presented around the *K* point for the graphene-derived (1 × 1) Brillouin zone. The weight of the graphene-derived p_z character is highlighted by the size of the filled circles superimposed with the plot of the band structure.

modification of the adsorption geometry, caused by the reduction of Y concentration, the nature of the interaction between graphene and the metal valence band states is also modified. While graphene remains to be *n*-doped also for the gr/0.33ML-Y/Co(0001) and gr/0.25ML-Y/Co(0001) systems, hybridization between C-p_z states and Y-d_{z^2} is not realized (missed space overlap) (Figures 2c,d and S7−S9). Consequently, the linear dispersion of the graphene-derived bands is preserved with an energy gap at the Dirac point for both gr/Y/Co(0001) systems with 0.33- and 0.25ML of intercalated Y (see Figures 2c,d and S7). After intercalation of Y, the magnetic moment of graphene is significantly reduced. The presence of Y at the interface yields an increase of MAE in magnitude, which decreases together with the intercalant concentration. Finally, in the case of gr/0.25ML-Y/Co(0001), the easy axis changes its direction (Table 1).

As a further outcome of Y intercalation in the gr/Co(0001) interface, the formation of an ordered YCo_2(111) alloy underneath a graphene layer was considered. Bulk YCo_2 crystallizes in the cubic Laves (C15) structure (Figure S10), and it is a paramagnetic material (Figure S11a).[36,42,43] It was found that the (111) surface of YCo_2 becomes ferromagnetic, independent of its termination by Co or Y atoms, with large magnetic moments in the topmost Co layer (Figure S11b,c).[36,37] The calculated magnetic moments for the Co and Y atoms in different layers of the YCo_2(111) slab of different terminations are presented in Table S4, and one can see that they quickly decrease with distance from the surface, which is in a good agreement with previously published data.[36] Due to an uncertainty in the thickness of YCo_2, which can be formed in the experiment, we consider here two possibilities: (i) gr/1ML-YCo_2/Co(0001) and (ii) gr/bulk-like-YCo_2(111) slab. In each case, two possible terminations are taken into account: Y- and Co-terminated (111) slabs (Figures 1, S12, and S13).

The obtained results weakly depend on the alloy thickness and are defined by the composition of the interface layer. In the case of the Co-terminated interfaces, graphene adopts the *top*−*hcp* configuration with respect to the substrate (Figure 1e,g, Tables S5−S8). These results are very similar to that of gr/Co(0001): Followed by the initial charge transfer from Co to graphene, the formation of the [C^{top}-p_z + M(S)-d_{z^2}] and [C^{fcc}-p_z + M(S)-d_{xz}, -d_{yz}] hybrid states destroys the linear dispersion relation of graphene (Figures 3a,c, S14, S15, S17, and S18). Due to the interaction between the graphene-π and Co 3d states, the graphene is weakly magnetized (m_C is about ±0.02 μ_B). The magnetic moment of the interface Co is 1.27 μ_B, while the magnetic moment of Co in the inner layers of the slab is close to zero. Furthermore, these two systems with a Co-terminated YCo_2(111) surface show larger in-plane anisotropy (1.38 and 0.58 meV/u.c., respectively) (Table 1).

In the case of the Y-terminated gr/YCo_2 interfaces, the energetically most favorable structures correspond to the *fcc*−*hcp* configuration with respect to the substrate (Figure 1f,h, Tables S5−S8). The further observations are comparable to those of the gr/0.25ML-Y/Co(0001) system, which has the same concentration of Y atoms at the interface as the Y-terminated YCo_2(111) slab. In the case of gr/1ML-YCo_2/Co(0001) and gr/bulk-like-YCo_2(111), only [C^{fcc}-p_z + M(S)-d_{xz}, -d_{yz}] hybrid states can be formed, which does not lead to the rearrangement of bands but to an opening of a band gap of about 0.35 eV with $E_D - E_F \approx -1.2$ eV for gr/YCo_2(111)

https://doi.org/10.1021/acsomega.1c07136
ACS Omega 2022, 7, 7304−7310

(Figures 3b,d, S14, S16, S17, and S19). As for the other systems under consideration, graphene is *n*-doped. Similarly to the results obtained for gr/0.25ML-Y/Co(0001), the magnetic moment of C atoms does not exceed 0.001 μ_B. The outermost Co in gr/1ML-YCo_2/Co(0001) and gr/bulk-like-YCo_2(111) has a rather high magnetic moment equal to 1.28 and 1.11 μ_B, respectively. At the same time, the magnetic moments of Co atoms in the middle layers of the YCo_2 slab are close to zero. Against the background of all this similarity, the two systems under discussion demonstrate different directions of easy axis: it lies in-plane in the case of gr/1ML-YCo_2/Co(0001) and out-of-plane in the case of gr/bulk-like-YCo_2(111).

CONCLUSIONS

In summary, we present the systematic DFT analysis of the crystallographic, magnetic, and electronic properties of different graphene/Y/Co(0001) interfaces. In the case of the sharp interfaces between all components, the *n*-doping level of graphene in the intercalation-like system strongly depends on the Y atoms' concentration, and in all cases, the formation of the band gap directly at the Dirac point is found for the graphene-derived π band. Such an effect is assigned to the hybridization of the respective valence band states of Y and graphene. For the more realistic case of the YCo_2 alloy formation at the interface, the graphene-protected ferromagnetic layer of the Y/Co alloy is formed either on ferromagnetic Co(0001) or on paramagnetic bulk alloy (independent of the termination by Y or Co atoms). In such a case, the electronic structure of a graphene layer strongly depends on the termination of a formed YCo_2 layer: for the Co-terminated or Y-terminated interfaces, it is similar to the cases of the graphene adsorption on bulk Co(0001) or on 0.25ML-Y/Co(0001), respectively. The obtained results for the modification of the electronic structure of graphene adsorbed on different Y/Co systems are in agreement with the general scheme used for the description of the graphene/metal interfaces, and these results are important for the engineering of the graphene-based interfaces, which can further be used in different electronics and spintronics applications.

COMPUTATIONAL DETAILS

Spin-polarized DFT calculations based on plane-wave basis sets of 500 eV cutoff energy were performed with the Vienna *ab initio* simulation package (VASP).[44−46] The Perdew−Burke−Ernzerhof (PBE) exchange-correlation functional[47] was employed. The electron−ion interaction was described within the projector augmented wave (PAW) method[48] with C (2s,2p), Co (3d,4s), and Y (4d,5s) states treated as valence states. The Brillouin zone integration was performed on Γ-centered symmetry reduced Monkhorst−Pack meshes using a Methfessel−Paxton smearing method of first order with σ = 0.15 eV, except for the calculation of total energies. For these calculations, the tetrahedron method with Blöchl corrections[49] was employed. The *k* mesh for sampling the supercell Brillouin zone was chosen to be as dense as at least 24 × 24 when folded up to the simple graphene unit cell. Dispersion interactions were included by means of the DFT-D3 correction method.[50] During structure optimization, the convergence criteria for energy was set equal to 10^{-5} eV. The band structures calculated for the studied systems were unfolded (if necessary) to the graphene (1 × 1) primitive unit cell according to the procedure described in refs 51 and 52 with the code BandUP.

The interfaces are modeled by a symmetrical slab composed of 23 layers of Co atoms in parent gr/Co(0001). In the case of the gr/Y/Co(0001) systems, the outer Co on both ends of the Co(0001) slab is replaced by one Y layer. For the YCo_2(111) surface, we used a repeated periodic slab geometry with up to 41 (43 with Y cap) layers of Y and Co atoms per slab. In all cases, graphene is adsorbed both on the top and bottom side of the slab with a vacuum gap of at least 20 Å (see Figure S20 for details). During structure relaxation, the *z*-coordinate positions of all carbon and yttrium atoms as well as those of the top and bottom three layers of the Co(0001) layer are relaxed until forces became smaller than 0.02 eV/Å. In order to describe the surface magnetism of the YCo_2(111) alloy, the *x*-, *y*-, and *z*-coordinate positions of the Co and Y atoms in the outer 6 layers were relaxed.

ASSOCIATED CONTENT

Supporting Information

The Supporting Information is available free of charge at https://pubs.acs.org/doi/10.1021/acsomega.1c07136.

Additional theoretical results for the following systems: graphene/Co(0001), graphene/Y/Co(0001), graphene/1ML-YCo_2/Co(0001), and graphene/bulk-like-YCo_2(111) (PDF)

AUTHOR INFORMATION

Corresponding Authors

Yuriy Dedkov − *Department of Physics, Shanghai University, 200444 Shanghai, P. R. China;* orcid.org/0000-0001-7904-2892; Email: yuriy.dedkov@icloud.com

Elena Voloshina − *Department of Physics, Shanghai University, 200444 Shanghai, P. R. China;* orcid.org/0000-0002-1799-1125; Email: elena.voloshina@icloud.com

Authors

Wenxuan Yue − *Department of Physics, Shanghai University, 200444 Shanghai, P. R. China*

Qilin Guo − *Department of Physics, Shanghai University, 200444 Shanghai, P. R. China*

Complete contact information is available at: https://pubs.acs.org/10.1021/acsomega.1c07136

Notes

The authors declare no competing financial interest.

ACKNOWLEDGMENTS

This work was supported by the National Natural Science Foundation of China (Grant No. 21973059). We appreciate the High Performance Computing Centre of Shanghai University and Shanghai Engineering Research Centre of Intelligent Computing System (No. 19DZ2252600) for providing the computing resources and technical support.

REFERENCES

(1) Geim, A. K.; Novoselov, K. S. The Rise of Graphene. *Nat. Mater.* **2007**, *6*, 183−191.

(2) Castro Neto, A. H.; Guinea, F.; Peres, N. M. R.; Novoselov, K. S.; Geim, A. K. The Electronic Properties of Graphene. *Rev. Mod. Phys.* **2009**, *81*, 109−162.

(3) Das Sarma, S.; Adam, S.; Hwang, E. H.; Rossi, E. Electronic Transport in Two-Dimensional Graphene. *Rev. Mod. Phys.* **2011**, *83*, 407−470.

(4) Andrei, E. Y.; MacDonald, A. H. Graphene Bilayers With a Twist. *Nat. Mater.* **2020**, *19*, 1265−1275.
(5) Novoselov, K. S.; Fal'ko, V. I.; Colombo, L.; Gellert, P. R.; Schwab, M. G.; Kim, K. A Roadmap for Graphene. *Nature* **2012**, *490*, 192−200.
(6) Ferrari, A. C.; Bonaccorso, F.; Fal'ko, V.; Novoselov, K. S.; Roche, S.; Bøggild, P.; Borini, S.; Koppens, F. H. L.; Palermo, V.; et al. Science and Technology Roadmap for Graphene, Related Two-Dimensional Crystals, and Hybrid Systems. *Nanoscale* **2015**, *7*, 4598−4810.
(7) Batzill, M. The Surface Science of Graphene: Metal Interfaces, CVD Synthesis, Nanoribbons, Chemical Modifications, and Defects. *Surf. Sci. Rep.* **2012**, *67*, 83−115.
(8) Dedkov, Y.; Voloshina, E. Graphene Growth and Properties on Metal Substrates. *J. Phys.: Condens. Matter* **2015**, *27*, 303002.
(9) Voloshina, E. N.; Dedkov, Y. S. General Approach to Understanding the Electronic Structure of Graphene on Metals. *Mater. Res. Express* **2014**, *1*, No. 035603.
(10) Yang, M.; Liu, Y.; Fan, T.; Zhang, D. Metal-Graphene Interfaces in Epitaxial and Bulk Systems: A Review. *Prog. Mater. Sci.* **2020**, *110*, 100652.
(11) Dedkov, Y.; Voloshina, E. Epitaxial Graphene/Ge Interfaces: A Minireview. *Nanoscale* **2020**, *12*, 11416−11426.
(12) Vita, H.; Böttcher, S.; Horn, K.; Voloshina, E. N.; Ovcharenko, R. E.; Kampen, T.; Thissen, A.; Dedkov, Y. S. Understanding the Origin of Band Gap Formation in Graphene on Metals: Graphene on Cu/Ir(111). *Sci. Rep.* **2015**, *4*, 5704.
(13) Voloshina, E.; Berdunov, N.; Dedkov, Y. Restoring a Nearly Free-Standing Character of Graphene on Ru(0001) by Oxygen Intercalation. *Sci. Rep.* **2016**, *6*, 20285.
(14) Voloshina, E.; Dedkov, Y. Realistic Large-Scale Modeling of Rashba and Induced Spin-Orbit Effects in Graphene/High-*Z*-Metal Systems. *Adv. Theory Simul.* **2018**, *1*, 1800063.
(15) Vincent, T.; Voloshina, E.; Pons, S.; Simon, S.; Fonin, M.; Wang, K.; Paulus, B.; Roditchev, D.; Dedkov, Y.; Vlaic, S. Quantum Well States for Graphene Spin-Texture Engineering. *J. Phys. Chem. Lett.* **2020**, *11*, 1594−1600.
(16) Wang, K.; Vincent, T.; Bouhiron, J. B.; Pons, S.; Roditchev, D.; Simon, S.; Fonin, M.; Paulus, B.; Dedkov, Y.; Vlaic, S.; et al. Influence of Surface and Subsurface Co−Ir Alloy on the Electronic Properties of Graphene. *Carbon* **2021**, *183*, 251−258.
(17) Weser, M.; Rehder, Y.; Horn, K.; Sicot, M.; Fonin, M.; Preobrajenski, A. B.; Voloshina, E. N.; Goering, E.; Dedkov, Y. S. Induced Magnetism of Carbon Atoms at the Graphene/Ni(111) Interface. *Appl. Phys. Lett.* **2010**, *96*, No. 012504.
(18) Weser, M.; Voloshina, E. N.; Horn, K.; Dedkov, Y. S. Electronic Structure and Magnetic Properties of the Graphene/Fe/Ni(111) Intercalation-Like System. *Phys. Chem. Chem. Phys.* **2011**, *13*, 7534−7539.
(19) Matsumoto, Y.; Entani, S.; Koide, A.; Ohtomo, M.; Avramov, P. V.; Naramoto, H.; Amemiya, K.; Fujikawa, T.; Sakai, S. Spin Orientation Transition Across the Single-Layer Graphene/Nickel Thin Film Interface. *J. Mater. Chem. C* **2013**, *1*, 5533−5537.
(20) Marchenko, D.; Varykhalov, A.; Sánchez-Barriga, J.; Rader, O.; Carbone, C.; Bihlmayer, G. Highly Spin-Polarized Dirac Fermions at the Graphene/Co Interface. *Phys. Rev. B* **2015**, *91*, 235431.
(21) Usachov, D.; Fedorov, A.; Otrokov, M. M.; Chikina, A.; Vilkov, O.; Petukhov, A.; Rybkin, A. G.; Koroteev, Y. M.; Chulkov, E. V.; Adamchuk, V. K.; et al. Observation of Single-Spin Dirac Fermions at the Graphene/Ferromagnet Interface. *Nano Lett.* **2015**, *15*, 2396−2401.
(22) Rougemaille, N.; N'Diaye, A. T.; Coraux, J.; Vo-Van, C.; Fruchart, O.; Schmid, A. K. Perpendicular Magnetic Anisotropy of Cobalt Films Intercalated Under Graphene. *Appl. Phys. Lett.* **2012**, *101*, 142403.
(23) Decker, R.; Brede, J.; Atodiresei, N.; Caciuc, V.; Blügel, S.; Wiesendanger, R. Atomic-Scale Magnetism of Cobalt-Intercalated Graphene. *Phys. Rev. B* **2013**, *87*, No. 041403.
(24) Vu, A. D.; Coraux, J.; Chen, G.; N'Diaye, A. T.; Schmid, A. K.; Rougemaille, N. Unconventional Magnetisation Texture in Graphene/Cobalt Hybrids. *Sci. Rep.* **2016**, *6*, 24783.
(25) Sun, X.; Pratt, A.; Yamauchi, Y. First-Principles Study of the Structural and Magnetic Properties of Graphene on a Fe/Ni(111) Surface. *J. Phys. D: Appl. Phys.* **2010**, *43*, 385002.
(26) Dedkov, Y. S.; Shikin, A. M.; Adamchuk, V. K.; Molodtsov, S. L.; Laubschat, C.; Bauer, A.; Kaindl, G. Intercalation of Copper Underneath a Monolayer of Graphite on Ni(111). *Phys. Rev. B* **2001**, *64*, No. 035405.
(27) Varykhalov, A.; Scholz, M. R.; Kim, T. K.; Rader, O. Effect of Noble-Metal Contacts on Doping and Band Gap of Graphene. *Phys. Rev. B* **2010**, *82*, 121101.
(28) Zhou, G.; Wang, P.; Li, H.; Hu, B.; Sun, Y.; Huang, R.; Liu, L. Spin-State Reconfiguration Induced by Alternating Magnetic Field for Efficient Oxygen Evolution Reaction. *Nat. Commun.* **2021**, *12*, 4827.
(29) Omiciuolo, L.; Hernández, E. R.; Miniussi, E.; Orlando, F.; Lacovig, P.; Lizzit, S.; Menteş, T. O.; Locatelli, A.; Larciprete, R.; Bianchi, M.; et al. Bottom-Up Approach for the Low-Cost Synthesis of Graphene-Alumina Nanosheet Interfaces Using Bimetallic Alloys. *Nat. Commun.* **2014**, *5*, 5062.
(30) Dedkov, Y.; Voloshina, E. Spectroscopic and DFT Studies of Graphene Intercalation Systems on Metals. *J. Electron Spectrosc. Relat. Phenom.* **2017**, *219*, 77−85.
(31) Jugovac, M.; Genuzio, F.; Menteş, T. O.; Locatelli, A.; Zamborlini, G.; Feyer, V.; Schneider, C. M. Tunable Coupling by Means of Oxygen Intercalation and Removal at the Strongly Interacting Graphene/Cobalt Interface. *Carbon* **2020**, *163*, 341−347.
(32) Voloshina, E.; Guo, Q.; Paulus, B.; Böttcher, S.; Vita, H.; Horn, K.; Zhao, C.; Cui, Y.; Dedkov, Y. Electronic Structure and Magnetic Properties of Graphene/Ni_3Mn/Ni(111) Trilayer. *J. Phys. Chem. C* **2019**, *123*, 4994−5002.
(33) Voloshina, E.; Dedkov, Y. Dirac Electron Behavior for Spin-Up Electrons in Strongly Interacting Graphene on Ferromagnetic Mn_5Ge_3. *J. Phys. Chem. Lett.* **2019**, *10*, 3212−3216.
(34) Guo, Q.; Dedkov, Y.; Voloshina, E. Intercalation of Mn in Graphene/Cu(111) Interface: Insights to the Electronic and Magnetic Properties From Theory. *Sci. Rep.* **2020**, *10*, 21684.
(35) Voloshina, E.; Paulus, B.; Dedkov, Y. Graphene Layer Morphology as an Indicator of the Metal Alloy Formation at the Interface. *J. Phys. Chem. Lett.* **2021**, *12*, 19−25.
(36) Khmelevskyi, S.; Mohn, P.; Redinger, J.; Weinert, M. Magnetism on the Surface of the Bulk Paramagnetic Intermetallic Compound YCo_2. *Phys. Rev. Lett.* **2005**, *94*, 146403.
(37) Dedkov, Y. S.; Laubschat, C.; Khmelevskyi, S.; Redinger, J.; Mohn, P.; Weinert, M. YCo_2: Intrinsic Magnetic Surface of a Paramagnetic Bulk Material. *Phys. Rev. Lett.* **2007**, *99*, No. 047204.
(38) Eom, D.; Prezzi, D.; Rim, K. T.; Zhou, H.; Lefenfeld, M.; Xiao, S.; Nuckolls, C.; Hybertsen, M. S.; Heinz, T. F.; Flynn, G. W. Structure and Electronic Properties of Graphene Nanoislands on Co(0001). *Nano Lett.* **2009**, *9*, 2844−2848.
(39) Khomyakov, P. A.; Giovannetti, G.; Rusu, P. C.; Brocks, G.; van den Brink, J.; Kelly, P. J. First-Principles Study of the Interaction and Charge Transfer Between Graphene and Metals. *Phys. Rev. B* **2009**, *79*, 195425.
(40) Voloshina, E.; Dedkov, Y. Electronic and Magnetic Properties of the Graphene-Ferromagnet Interfaces: Theory vs. Experiment. In *Physics and applications of graphene - experiments*; Mikhailov, S., Ed.; InTech, 2011; pp 329−351.
(41) Xiao, R.; Fritsch, D.; Kuzmin, M. D.; Koepernik, K.; Eschrig, H.; Richter, M.; Vietze, K.; Seifert, G. Co Dimers on Hexagonal Carbon Rings Proposed as Subnanometer Magnetic Storage Bits. *Phys. Rev. Lett.* **2009**, *103*, 187201.
(42) Goto, T.; Fukamichi, K.; Sakakibara, T.; Komatsu, H. Itinerant Electron Metamagnetism in YCo_2. *Solid State Commun.* **1989**, *72*, 945−947.
(43) Khmelevskyi, S.; Turek, I.; Mohn, P. Formation of a Weak Ferromagnetic State in $Y(Co_{1-x}Al_x)_2$ Compounds: A Coherent

https://doi.org/10.1021/acsomega.1c07136
ACS Omega 2022, 7, 7304−7310

Potential Approximation Study. *J. Phys.: Condens. Matter* **2001**, *13*, 8405.
(44) Kresse, G.; Hafner, J. Ab Initio Molecular Dynamics For Liquid Metals. *Phys. Rev. B* **1993**, *47*, 558−561.
(45) Kresse, G.; Hafner, J. Norm-Conserving and Ultrasoft Pseudopotentials for First-Row and Transition Elements. *J. Phys.: Condens. Matter* **1994**, *6*, 8245.
(46) Kresse, G.; Furthmüller, J. Efficiency of Ab-Initio Total Energy Calculations for Metals and Semiconductors Using a Plane-Wave Basis Set. *Comput. Mater. Sci.* **1996**, *6*, 15−50.
(47) Perdew, J. P.; Burke, K.; Ernzerhof, M. Generalized Gradient Approximation Made Simple. *Phys. Rev. Lett.* **1996**, *77*, 3865−3868.
(48) Blöchl, P. E. Projector Augmented-Wave Method. *Phys. Rev. B* **1994**, *50*, 17953−17979.
(49) Blöchl, P. E.; Jepsen, O.; Andersen, O. K. Improved Tetrahedron Method For Brillouin-Zone Integrations. *Phys. Rev. B* **1994**, *49*, 16223−16233.
(50) Grimme, S.; Antony, J.; Ehrlich, S.; Krieg, H. A Consistent and Accurate Ab Initio Parametrization of Density Functional Dispersion Correction (DFT-D) for the 94 Elements H-Pu. *J. Chem. Phys.* **2010**, *132*, 154104.
(51) Medeiros, P. V. C.; Stafström, S.; Björk, J. Effects of Extrinsic and Intrinsic Perturbations on the Electronic Structure of Graphene: Retaining an Effective Primitive Cell Band Structure By Band Unfolding. *Phys. Rev. B* **2014**, *89*, No. 041407.
(52) Medeiros, P. V. C.; Tsirkin, S. S.; Stafström, S.; Björk, J. Unfolding Spinor Wave Functions and Expectation Values of General Operators: Introducing the Unfolding-Density Operator. *Phys. Rev. B* **2015**, *91*, No. 041116.

https://doi.org/10.1021/acsomega.1c07136
ACS Omega 2022, 7, 7304−7310